

PROPAGATION OF UNCERTAINTY IN A TRANSMISSION LINE GUYED TOWER WITH STOCHASTIC GUY PRETENSION AND SUBJECTED TO WIND LOAD

Bruno J. Rango^a, Marta B. Rosales^a, Jorge S. Ballaben^b, Roberta Lima^c and Rubens Sampaio^c

^a*Department of Engineering, Universidad Nacional del Sur, Alem 1253, 8000 Bahía Blanca and IFISUR (UNS-CONICET), Argentina, brunorango@gmail.com, mrosales@criba.edu.ar*

^b*Department of Engineering, Universidad Nacional del Sur, Alem 1253, 8000 Bahía Blanca and CONICET, Argentina, jorgeballaben@gmail.com*

^c*Mechanical Engineering Department, PUC-Rio, Rio de Janeiro, RJ, Brazil, robertalima@puc-rio.br, rsampaio@puc-rio.br*

Keywords: Transmission lines, guyed tower, wind load, stochastic pretension

Abstract. Guyed transmission lines are extensively used in overhead power transmission around the world. This kind of structures presents a series of favorable characteristics like simple installation procedure, low weight and low cost. However, on the other side, they are highly flexible, and exhibit a very nonlinear behavior. Moreover, the most demanding load is represented by wind, which is of random nature. In this sense, the present study addresses the dynamic analysis of a three-dimensional model of a transmission line segment composed by a guyed tower with four guy wires and two spans of conductor cables, subjected to stochastic wind load. The model accounts for the coupling effect between the different physics that take place. In this scheme, the supporting tower is modeled as a linear equivalent beam-column, assuming the hypothesis of the Euler-Bernoulli beam theory and with properties equivalent to a lattice tower. The second order effect due to axial loads on the tower is considered. The motion of the conductors and the guys, on the other side, is governed by a set of nonlinear equations which considers the cables extensibility. The system is discretized by means of the Finite Element Method. The wind velocity comprises a mean and a turbulent component. The Spectral Representation Method is used to derive the latter, which starts from a Power Spectral Density of the wind velocity leading to a function that accounts for both the temporal and spatial correlations. In order to assess the sensitivity of the structure to the variations of the stiffness, the initial tension in each of the four guy cables is assumed an independent random variable. Given the available information about the pretension variables, the Principle of Maximum Entropy is applied to derive the corresponding probability distributions. The stochastic response of the structure is evaluated.

1 INTRODUCTION

Guyed transmission towers present a series of favorable characteristics which makes them suitable for overhead electric transmission. A typical configuration of the *suspension* type is shown in Fig. 1. In effect, they are cheaper and lighter than traditional self-supporting towers and their field assemblage procedure is simpler. On the other side, this kind of structures are very flexible, their stability is strongly dependent on the tension of the guy cables, and their overall behavior is highly nonlinear. Moreover, the most demanding load is represented by the wind, which is random in nature. As a result, the response of the transmission line to the load is random as well.

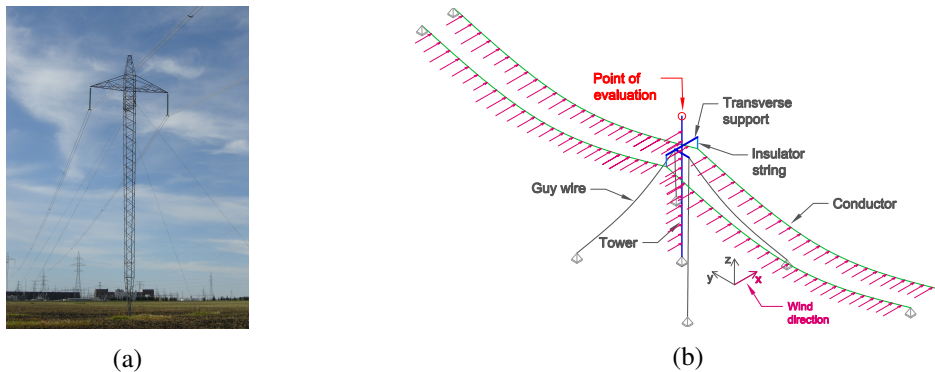


Figure 1: (a) Photograph of a transmission guyed tower of suspension-type. (b) Scheme of the simplified model of the guyed transmission line segment under study.

Because of the mentioned characteristics, the dynamic behavior of flexible guyed structures subjected to wind load constitutes a matter of active research. Gani and Legeron (2010), for instance, present a comparison between the response of a 3D model of a transmission line segment subjected to the static-equivalent wind load proposed in the international standard IEC 60826 and the transient dynamic response of the structure under a simulated stochastic wind load field. They perform 10 realizations of the stochastic problem and compute the average of the maximum peaks of the resulting stochastic processes of interest. The authors conclude that the static-equivalent method not always provides conservative results.

The pretension of the guys, which is defined at the design stage, plays a very important role in the dynamic behavior of flexible guyed structures. The relevance of this issue is addressed by Ballaben et al. (2017). However, at the moment of the tower assemblage, this magnitude is installed within certain error margins, and furthermore, it will inevitably vary during the lifespan of the structure. Moreover, predominant directions of wind, for instance, can cause unequal softening of the guys. For these reasons, the consideration of the guys pretension as an independent random variable seems an adequate approach.

The present study addresses the uncovered probabilistic evaluation of the dynamic response of a guyed transmission line with uncertain pretension of the guys, subjected to stochastic wind load. The turbulent component of the wind speed is assumed to be characterized by the spectrum proposed by Davenport (1961). The spatial and temporal correlations of this component are accounted for. Furthermore, the wind load according to the IEC 60826 code is also considered.

A mathematical model of a guyed transmission tower and two adjacent spans of conductors in the 3D space is stated. The cable elements (*i.e.* guy wires, insulator strings, and conductors) are modeled according to the nonlinear formulation proposed by Luongo et al. (1984). The lat-

tice tower, on the other side, is simplified as an equivalent column assuming the Euler-Bernoulli beam theory. The coupled nonlinear system of equations is discretized through the Finite Element Method. The stochastic wind speed field for the wind load is generated by means of the Spectral Representation Method (SRM). The pretensions of the four guys are assumed as independent and identically distributed random variables. The Principle of Maximum Entropy (PME) is applied to derive the corresponding density functions.

A series of Monte Carlo simulations of the dynamic response of the stochastic discretized system are performed. The study focuses on three stochastic processes of the system response: the dynamic tension of the windward guy cables, and the displacements in the direction of the wind at the top of the tower. In particular, the random first passage of these processes through the reference threshold defined by the static response of the structure under the IEC 60826 wind load is assessed.

2 DETERMINISTIC MATHEMATICAL MODEL

A scheme of the transmission line model under study is represented in Fig. 1. The supporting tower is composed by a latticed main vertical tower of 52.18 m height, two transverse support of 6.71 m length from which the insulator chains hung, and four guy wires which are connected to the tower at 38.04 m from its base. The latticed elements are modeled as beams-columns. Two spans of 480 m of conductor cables are considered for the study. The conductors are connected to the insulator strings from one side and a pinned condition is assumed on their other end.

A mathematical model in the 3D-space is stated. The vertical tower and the transverse support are modeled assuming the Euler-Bernoulli beam theory. Moreover, the axial and torsional deformations of the beam are considered, and the stress-strain relations are assumed linear. On the other side, the conductors, guy wires, and insulator strings are modeled as elastic unidimensional cables, by means of the nonlinear formulation proposed by Luongo et al. (1984). In this scheme, the following hypothesis are adopted: (i) the stress-strain relation is assumed linear, (ii) the flexural, torsional, and shear rigidities are neglected, (iii) the axial deformations of the cable are described through the Lagrangian strain measure, and (iv) the static equilibrium configuration is represented by a parabolic profile. This assumption is valid for taut cables, where the sag to span ratio is less or equal than 1/10, which is the case of the cables in this work. The displacements of the cable during its motion are referred to the initial parabolic profile.

The weak form of the governing equations reads:

$$m(\ddot{\mathbf{v}}, \boldsymbol{\phi}) + c(\dot{\mathbf{v}}, \boldsymbol{\phi}) + k(\mathbf{v}, \boldsymbol{\phi}) + bc(\mathbf{v}, \boldsymbol{\phi}) = f(\mathbf{v}, \boldsymbol{\phi}) \quad (1)$$

In Eq. 1, $m(\ddot{\mathbf{v}}, \boldsymbol{\phi})$, $c(\dot{\mathbf{v}}, \boldsymbol{\phi})$, and $k(\mathbf{v}, \boldsymbol{\phi})$ denote the mass, damping, and stiffness operators, respectively, and $bc(\mathbf{v}, \boldsymbol{\phi})$, $f(\mathbf{v}, \boldsymbol{\phi})$ are the boundary conditions and external forces operators, respectively. From now on, sub-indexes b and c stand for the beam and the cable elements, respectively. The field variables are $\mathbf{v} = u_b, v_b, w_b, \theta_x$ for the beam and $\mathbf{v} = \{u_c, v_c, w_c\}$ for the cable. The vector of admissible weight functions is represented by $\boldsymbol{\phi} = \{\phi_b, \phi_c\}$. The displacements along the local $\{x_{b,c}, y_{b,c}, z_{b,c}\}$ directions are $\{u_{b,c}, v_{b,c}, w_{b,c}\}$, and θ_x is the twist angle of the beam around its longitudinal (x_b) axis. The external actions per unit length on the beam and cable are $\{q_{xb}, q_{yb}, q_{zb}, m_{xb}\}$ and $\{q_{xc}, q_{yc}, q_{zc}\}$, respectively. Thus, the expressions

for the operators in Eq. 1, are:

$$\begin{aligned}
 m(\ddot{\mathbf{v}}, \phi) &= \int_0^{l_b} \phi_b m_b (\ddot{u}_b + \ddot{v}_b + \ddot{w}_b) dx_b + \int_0^{l_c} \phi_c m_c (\ddot{u}_c + \ddot{v}_c + \ddot{w}_c) dx_c \\
 c(\dot{\mathbf{v}}, \phi) &= \int_0^{l_b} \phi_b c_b (\dot{u}_b + \dot{v}_b + \dot{w}_b) dx_b + \int_0^{l_c} \phi_c c_c (\dot{u}_c + \dot{v}_c + \dot{w}_c) dx_c \\
 k(\mathbf{v}, \phi) &= \int_0^{l_b} [e_b (i_z v_b'' + i_y w_b'') \phi_b'' + e_b a_b u_b' \phi_b' + g_b i_x \theta_x' \phi_b' + n_b (v_b' + w_b') \phi_b'] dx_b + \\
 &\quad + \int_0^{l_c} [\phi_c' h (v_c' + w_c') + \phi_c' e_c a_c (y_c' + v_c') \varepsilon + \phi_c' e_c a_c \varepsilon] dx_c \\
 bc(\mathbf{v}, \phi) &= e_b i_z v_b''' \phi|_0^{l_b} + e_b i_y w_b''' \phi|_0^{l_b} - e_b i_z v_b'' \phi'|_0^{l_b} - e_b i_y w_b'' \phi'|_0^{l_b} + n_b v_b' \phi|_0^{l_b} + n_b w_b' \phi|_0^{l_b} + \\
 &\quad + e_b a_b u_b' \phi|_0^{l_b} + g_b i_x \theta_x' e_b a_b u_b' \phi|_0^{l_b} + h v_c' \phi|_0^{l_c} + h w_c' \phi|_0^{l_c} + e_c a_c (y_c' + v_c') \varepsilon h \phi|_0^{l_c} \\
 f(\mathbf{v}, \phi) &= \int_0^{l_b} \phi_b (q_{xb} + q_{yb} + q_{zb} + m_{xb}) dx_b + \int_0^{l_c} \phi_c (q_{xc} + q_{yc} + q_{zc}) dx_c
 \end{aligned} \tag{2}$$

where n_b is the axial load acting on the beam. The cross section area, mass per unit length, damping, and modulus of elasticity of the beam and cable are represented by $a_{b,c}$, $m_{b,c}$, $c_{b,c}$, and $e_{b,c}$, respectively. The shear modulus of the beam is denoted g_b , whereas its second moments of area with respect to the three local axes are i_x , i_y , and i_z . The elongation of the cable is expressed by $\varepsilon = u_c' + y_c' v_c' + 1/2 v_c'^2$. Denoting s_c as the cable sag, the equation of the parabola which describes the initial configuration of static equilibrium under self weight is $y_c = 4s_c [x_c/l_c - (x_c/l_c)^2]$. The parameter h represents the pretension of the cable. The geometric and mechanical properties considered for the study are reported in Tables 1 and 2.

	a_b [m ²]	i_y [m ⁴]	i_z [m ⁴]	i_x [m ⁴]	m_b [kg/m]	e_b [N/m ²]	g_b [N/m ²]
Tower	3.71×10^{-3}	2.62×10^{-3}	2.62×10^{-3}	5.20×10^{-3}	41.92	2.00×10^{11}	8.50×10^{10}

Table 1: Geometrical and mechanical properties of the tower modeled as an equivalent beam.

	d_c [mm]	m_c [kg/m]	e_c [N/m ²]
Guy cables	14.3	0.94	1.86×10^{11}
Conductors	40.6	2.95	0.62×10^{11}

Table 2: Diameter d_c and mechanical properties of the cables.

2.1 Finite Element Discretization

After deriving the weak form of the governing equations, the system is discretized by means of the Finite Element Method. In this sense, beam equations are discretized into 2-node linear elements of 12 DOFs (6 by node) whereas the cable equations are discretized into 3-node curved nonlinear elements of 9 DOFs (3 by node). After assembling the matrices, the system equation

results:

$$[m] \ddot{\mathbf{u}}(t) + [c] \dot{\mathbf{u}}(t) + [k] \mathbf{u}(t) + \mathbf{k}_{nl}(\mathbf{u}(t)) = \mathbf{f}(t) \quad (3)$$

where \mathbf{u} is the vector of DOF, $[m]$, $[c]$ are the mass and damping matrix, $[k_i]$ is the beam stiffness matrix, $\mathbf{k}_{nl}(\mathbf{u})$ is the nonlinear vector associated with the cable elements stiffness, and \mathbf{f} is the vector of external forces.

3 STOCHASTIC MODELS

3.1 Stochastic wind model

The action of wind on structures depends on the total wind speed $\mathcal{V}_T(z, t)$, which is random in nature. However, it can be divided in two parts, the deterministic mean wind speed, which varies with the height z above the ground, and the turbulent wind part which varies not only with height but also in time:

$$\mathcal{V}_T(z, t) = \mu_{v_T}(z) + \mathcal{V}(z, t) \quad (4)$$

The potential profile of the mean wind speed is $\mu_{v_T}(z) = v_0(z/10)^\alpha$. The term $v_0 = 38.75$ m/s represents the reference wind speed. This parameter depends on the geographical placement of the structure, and is provided by national standards. The value adopted in this work corresponds to the city of Bahia Blanca. For terrain category B, the exponent α assumes the value 0.16 (IEC 60826).

The characterization of the turbulent component, on the other side, is not that straightforward. It is defined by its power spectral density function (PSDF). In the present study, the spectrum proposed by Davenport (1961) is adopted:

$$\frac{s(z, \omega)\omega}{\sigma_v^2} = \frac{2}{3} \frac{f_l(z, \omega)^2}{(1 + f_l(z, \omega)^2)^{4/3}} \quad (5)$$

In this expression, $s(z, \omega)$ is the PSDF of the along-wind turbulence component, ω is the frequency, $\sigma_v = 6.6$ m/s is the standard deviation of the turbulent wind speed component, and $f_l(z, \omega) = \omega l_v / \mu_{v_T}(z)$ is a non-dimensional variable which depends on the frequency, the longitudinal integral length of the turbulence $l_v = 1200$ m, and the mean wind speed. The statistical dependence of the turbulence components at two separate points in the space, due to the spatial dimension of the wind vortices, is defined by the cross spectrum:

$$s^c(z_1, z_2, \omega) = s_{12}^c(\omega) = \sqrt{s(z_1, \omega)s(z_2, \omega)} \exp(-\gamma) \quad (6)$$

$$\gamma = \frac{2\omega[(c_y(y_2 - y_1))^2 + (c_z(z_2 - z_1))^2]^{1/2}}{[\mu_{v_T}(z_1) + \mu_{v_T}(z_2)]} \quad (7)$$

The coherence function γ involves the distance between the two points under consideration along the vertical ($z_2 - z_1$) and transverse-to-wind ($y_2 - y_1$) direction, affected by the respective non-dimensional decay coefficients $c_z=10$ and $c_y=16$ (Gani and Legeron, 2010).

On this basis, the Spectral Representation Method (SRM) (Shinozuka and Jan, 1972) allows to simulate the turbulent wind speed field. The wind is considered to act transversally to the conductors, in the direction of the x-axis (see Fig. 1). For the sake of brevity, the derivation of the method is not outlined. For a comprehensive description, the reader is referred to Ballaben

et al. (2017). In this scheme, the random wind speed registers $\mathcal{V}_j(z, t)$ $j = 1, \dots, m$ are generated at $m = 52$ points on the structure: 12 along the tower height and 20 points along each of both conductors spans placed in the windward yz plane. Since the variation of the wind speed in the along-wind distance between conductors is disregarded, the same wind speed is considered to act in both planes. These stochastic processes are simulated as a sum of cosines of random frequencies Ω_n and phase angles Φ_{kn} :

$$\mathcal{V}_j(z_j, t) = \sum_{k=1}^m \sum_{n=1}^{n_f} |h_{jk}(\omega_n)| \sqrt{2\Delta\omega} \cos[\Omega_n t + \Phi_{kn}] \quad (8)$$

For the simulations, a cutoff frequency of 4 Hz is defined and the spectrum is discretized into $n_f = 1000$ intervals of amplitude $\Delta\omega = 0.004$ Hz. Thus, every random frequency is defined as $\Omega_n = n\Delta\omega + \Psi_{kn}\Delta\omega$. Both the random parameter Ψ_{kn} and the independent random phase angles Φ_{kn} are uniformly distributed in the interval $[0, 2\pi]$. The time step and duration of the registers are defined as $dt = 0.125$ s and $t_f = 540$ s, respectively. The amplitude $|h_{jk}(\omega_n)|$ corresponds to the (j, k) entry in the lower triangular matrix $[h(\omega)]$, obtained as the Cholesky decomposition of the cross-spectral density matrix $[s(\omega)]$.

On this basis, the stochastic wind load field $\mathcal{F}_j(z, t)$ acting on the tower and conductors is computed as:

$$\mathcal{F}_j(z, t) = \frac{1}{2} \rho_a c_d a_w \mu_{vT}(z)^2 + \rho_a c_d a_w \mu_{vT}(z) \mathcal{V}_j(z, t) \quad (9)$$

where $\rho_a = 1.225$ kg/m³ is the air density, the drag coefficient c_d is 1 for conductors and 3.34 for the tower, and a_w is the area of the element exposed to the wind.

3.2 Guys random pretension model

The pretensions $h_{1,\dots,4}$ of the 4 guy cables are considered independent and identically distributed random variables, denoted H_1 and H_2 for the windward guys, and H_3 and H_4 for the leeward guy cables. For the characterization of their (identical) probability distribution, they will be all referred as H . For the model in this work, the mean of the random variable H is assumed as 10% of the cable UTF, i.e. $\mu_H = 13200$ N, and its standard deviation as 1/5 of the mean: $\sigma_H = 2640$ N. Moreover, it is known that this variable can not assume negative values, which establishes a lower margin for the support of the random variable. With this information, the application of the Principle of Maximum Entropy leads to a Gamma distribution of the random guy pretension with shape and scale parameters $\alpha = (\mu_H/\sigma_H)^2$ and $\beta = \sigma_H^2/\mu_H$, respectively:

$$H \sim \Gamma(a, b) = \frac{x^{a-1} e^{-\frac{x}{b}}}{\Gamma(a) b^a}; \quad h > 0 \quad (10)$$

4 EVALUATION OF THE STOCHASTIC RESPONSE

The inclusion of the stochastic wind load field and the random pretension of the guy cables in the mathematical model converts Eq. 3 into a discretized stochastic system of nonlinear equations. In order to derive a statistic model for the stochastic response, a series of Monte Carlo simulations of the discretized model are performed.

4.1 Computational implementation

Each numerical simulation of the system dynamics consists of two steps. First, the pretension of the guy cables is applied and the static configuration of equilibrium under self weight is

computed by means of the nonlinear Newton-Raphson solver. Thus, the initial configuration for the dynamic analysis of the system under wind load is obtained. Within the dynamic study, the discretized system of equations is integrated by means of a coupled Newmark/Newton-Raphson solver with a fixed time step of $\Delta t_{dyn} = 0.0313$ s. The structural damping matrix is constructed as linear combination of the mass and linearized stiffness matrices $[c] = \alpha_r[m] + \beta_r[k_l]$, being α_r and β_r the respective Rayleigh coefficients. These are computed separately for every structural element based on the corresponding damping ratio, namely $\epsilon_c = 0.001$ for conductors and guy cables and $\epsilon_c = 0.005$ for the tower (Gani and Legeron, 2010). In order to improve the stability of the dynamic solver, a sine window is applied to the wind load such that its full magnitude be progressively developed during the first minute of the simulation. This initial transient period and the successive 60 seconds are disregarded, and the remaining 7 minutes are analyzed.

4.2 Monte Carlo simulations

In this study, attention is focused on three stochastic processes: the dynamic tension of the two guy wires in the windward side, denoted as $\mathcal{H}1(t)$ and $\mathcal{H}2(t)$, and the displacements at the top of the tower (indicated as *point of evaluation* in Fig. 1) in the direction of the wind, denoted $\mathcal{U}(t)$. A convergence study is performed in order to determine the minimum number of Monte Carlo simulations of the problem that allow to construct representative statistics of the stochastic response. In this regard, the evolution with the number of realizations nr of the sample mean $\hat{\mu}_{\mathcal{X}}(t_p)$ and standard deviation $\hat{\sigma}_{\mathcal{X}}(t_p)$ of the processes (\mathcal{X} represents either $\mathcal{H}1$, $\mathcal{H}2$, or \mathcal{U}) in a particular time t_p is evaluated. Specifically, the coefficient of variation $\hat{\delta}_{\mathcal{X}}(t_p) = \hat{\mu}_{\mathcal{X}}(t_p)/\hat{\sigma}_{\mathcal{X}}(t_p)$ is computed. Figure 2a shows the convergence of this statistic for the three stochastic processes under study. It can be observed that after 2000 realizations of the problem, the coefficient of variation remains approximately stable, which suggests that convergence has been attained. Fig. 2b confirms that similar magnitudes of the coefficient of variation are obtained at every instant of time. Moreover, the latter graph suggests that the first order statistics do not vary with time. Besides this, in a previous study (Rango et al., 2018) it has been found that the sample correlation of the processes depend on one parameter only, *i.e.* the difference in time, and that the temporal mean coincides approximately with the sample mean. This is, it can be assumed that the processes are stationary and ergodic.

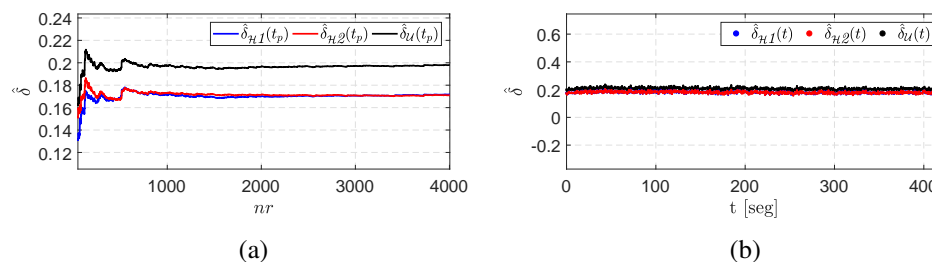


Figure 2: Convergence of the stochastic processes under study. (a) Evolution of the sample coefficient of variation $\hat{\delta}$, at a particular time t_p . (b) Sample coefficient of variation $\hat{\delta}$ at each simulated time t .

An interesting feature of the stochastic response arises from the construction of scatter plots of the dynamic tension on the windward (Fig. 3a) and leeward guy cables (Fig. 3b) at each instant during one particular realization. Indeed, a positive correlation is apparent between the tensions in the windward guy cables. On the other side, any particular trend is apparent in Fig. 3b. This suggests that, despite the initial independence in the guys pretension, the wind load

field induces a correlation between the dynamic tensions in the windward guy cables.

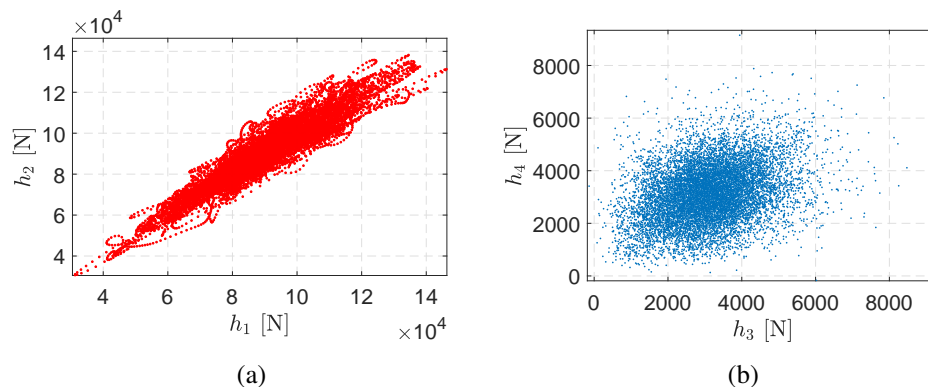


Figure 3: Dynamic tension of the (a) windward and (b) leeward guy cables at every instant during one particular realization of the problem.

4.3 Statistics of extremes

In this section, the extreme values of the stochastic processes $\mathcal{H}1(t)$, $\mathcal{H}2(t)$, and $\mathcal{U}(t)$, are considered. The maximum peak of these processes constitutes random variables that are denoted $H1_p$, $H2_p$, and U_p , respectively. Moreover, for comparative purposes, these distributions are compared with the static results from the application of the IEC 60826 static-equivalent wind load. For the static analysis, the pretension of the guy wires is defined as the mean of the associated random variable $\mu_H = 13200$ N. The deterministic value of the resulting tension force of the guy cables on the windward side and the displacement at the top of the tower are denoted as $h1_{st}$, $h2_{st}$, and u_{st} , respectively.

Figure 4(a)-(c) shows 4000 samples of the random variables $H1_p$, $H2_p$, and U_p , respectively. The horizontal red line indicates the reference threshold values $h1_{st}$, $h2_{st}$, and u_{st} . It can be observed that in the three cases, a series of samples exceed the static threshold. A particular realization could result in no surpasses of the reference value and, likewise, the limit could be exceeded once, or more than once. Attention will be focused now towards the statistical evaluation of the problem of level crossings (Lima and Sampaio, 2017).

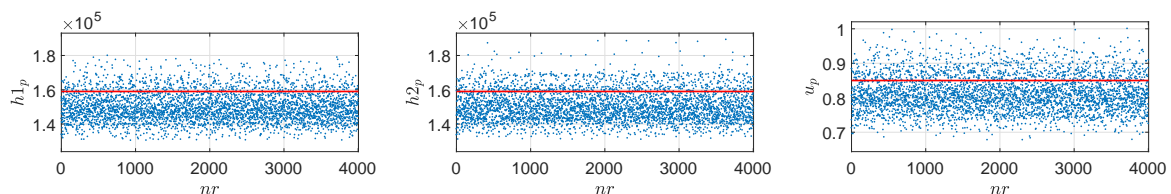


Figure 4: Realizations of the random variables $H1_p$, $H2_p$, and U_p , associated with the maximum value of the respective stochastic processes.

The random variable associated with the time of occurrence of the first passage of the random processes $\mathcal{H}1(t)$, $\mathcal{H}2(t)$, and $\mathcal{U}(t)$ beyond the reference threshold will be denoted as T_{h1} , T_{h2} , and T_u , respectively. Their normalized histograms, constructed with 596, 735, and 924 sample realizations, respectively, are reported in Fig. 5. The reason for the variability in the size of the sample lies in the fact that the number of realizations that exhibits at least one excursion

is a random variable as well. The higher distribution of probability near the beginning of the histograms suggests that the first passage is likely to occur relatively soon.

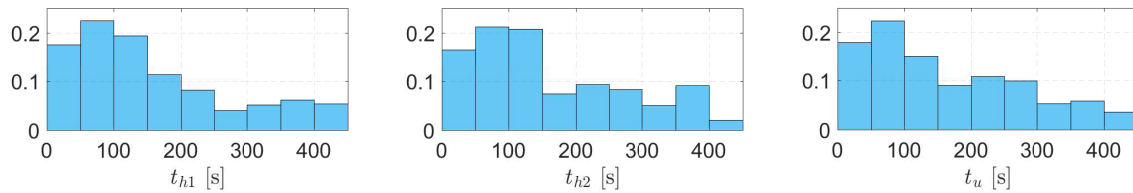


Figure 5: Normalized histograms of the random variables T_{h1} , T_{h2} , and T_u , constructed with 596, 735, and 924 samples, respectively.

The study is completed with an evaluation of the duration of the first passage. In this sense, three new random variables are defined, *i.e.* D_{h1} , D_{h2} , and D_u characterize the time elapsed between the first crossing with positive slope and the first crossing with negative slope of the stochastic processes $\mathcal{H}1(t)$, $\mathcal{H}2(t)$, and $\mathcal{U}(t)$ through the respective reference threshold. Their normalized histograms are reported in Fig. 6. The available number of samples of each random variable is the same as for T_{h1} , T_{h2} , and T_u , respectively. In the case of D_u , the normalized histogram could be associated with that of a Gamma distribution. This trend is not observable in the histograms of D_{h1} and D_{h2} .

Statistics of these random variables are reported in Table 3. Specifically, the sample mean, standard deviation (SD), coefficient of variation (COV), skewness, and kurtosis, are computed. From this information, it follows that the first passage occurs, in average, 3 minutes apart from the beginning of the processes. However, this random variables shows a relatively high dispersion, as indicated by the sample SD and COV. The average duration, on the other side, lies around 0.2 s for the three stochastic processes, and exhibits a lower dispersion of the samples results (see COV). The consideration of the first passage problem in stochastic processes is important. It constitutes the starting point towards the determination of reliability measures, which will be tackled by the authors in an upcoming work.

5 CONCLUSIONS

The present work addresses the statistical evaluation of the response of a guyed transmission line subjected to a stochastic wind load field and with the inclusion of uncertainty in the pretension of the guys. A series of Monte Carlo simulations of the structural response were performed. The study focuses on three stochastic processes of the structural response: the tension of the guy cables on the windward side, and the along-wind displacements at the top of the tower.

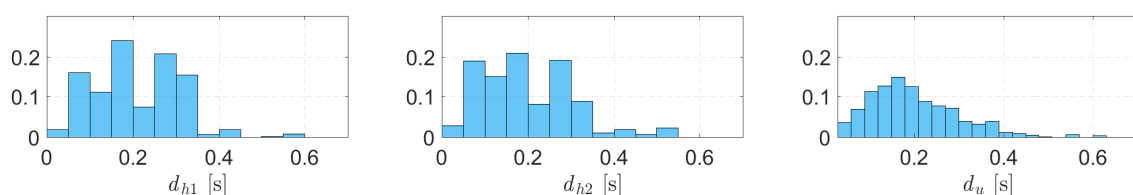


Figure 6: Normalized histograms of the random variables D_{h1} , D_{h2} , and D_u , constructed with 596, 735, and 924 samples, respectively.

	Mean	SD	COV	Skewness	Kurtosis
T_{h1}	162.46	114.82	0.71	0.59	2.20
T_{h2}	161.54	114.74	0.71	0.64	2.19
T_u	158.99	117.73	0.74	0.82	2.51
D_{h1}	0.21	0.10	0.48	0.59	3.46
D_{h2}	0.20	0.10	0.53	0.83	3.58
D_u	0.19	0.10	0.53	0.94	4.21

Table 3: Statistics of the random variables associated with the time of occurrence (T_{h1} , T_{h2} , T_u) and duration (D_{h1} , D_{h2} , D_u) of the first excursion of the random processes through their respective reference threshold.

It was found that during the interaction of the structure with the dynamic wind load, the initial independence of the random tension is lost in the windward guy cables, which exhibit a positive correlation. Moreover, the study showed that the static response of the structure under the static-equivalent wind load proposed in the IEC 60826 standard, is likely to be surpassed. Therefore, the random variables which characterize the time of occurrence and duration of the first of these passages, were studied. Indeed, normalized histograms and statistics were computed, and quantities as the average time of occurrence and duration of the first passage were reported.

ACKNOWLEDGMENTS

The authors acknowledge the support given by CONICET, MINCyT, and UNS (Argentina) and Faperj, and CNPq (Brazil).

REFERENCES

- Ballaben J., Guzmán A., and Rosales M. Nonlinear dynamics of guyed masts under wind load: Sensitivity to structural parameters and load models. *Journal of Wind Engineering and Industrial Aerodynamics*, 169:128–138, 2017.
- Davenport A. The spectrum of horizontal gustiness near the ground in high winds. *Quarterly Journal of the Royal Meteorological Society*, 87(372):194–211, 1961.
- Gani F. and Legeron F. Dynamic response of transmission lines guyed towers under wind loading. *Canadian Journal of Civil Engineering*, 37:450–464, 2010.
- IEC 60826. Design Criteria of Overhead Transmission Lines. International standard, International Electrotechnical Commission (IEC), Geneva, Switzerland, 2003.
- Lima R. and Sampaio R. Construction of a statistical model for the dynamics of a base-driven stick-slip oscillator. *Mechanical Systems and Signal Processing*, 91:157–166, 2017.
- Luongo A., Rega G., and Vestroni F. Planar non-linear free vibrations of an elastic cable. *International Journal of Non-Linear Mechanics*, 19(1):39–52, 1984.
- Rango B., Ballaben J., Sampaio R., and Rosales M. Uncertainty quantification in a transmission line guyed tower under wind load. *Proceedings of the ICVRAM-ISUMA UNCERTAINTIES 2018, Florianopolis, Brazil*, 2018.
- Shinozuka M. and Jan C. Digital simulation of random processes and its applications. *Journal of Sound and Vibration*, 25(1):111–128, 1972.